Mech. Sci., 2, 33–40, 2011
www.mech-sci.net/2/33/2011/
doi:10.5194/ms-2-33-2011

Mechanical Sciences
Open Access

Kinematic design of a finger abduction mechanism for an anthropomorphic robotic hand

L.-A. A. Demers and C. Gosselin

Département de génie mécanique, Université Laval, Québec, QC, G1V 0A6, Canada

Received: 25 February 2010 – Revised: 18 June 2010 – Accepted: 19 August 2010 – Published: 8 February 2011

Abstract. This paper presents the kinematic design of an abduction mechanism for the fingers of an underactuated anthropomorphic robotic hand. This mechanism will enhance the range of feasible grasps of the underactuated hand without significantly increasing its complexity. The analysis of the link between the index finger and the third finger is first assessed, where the parameters are studied in order to follow the amplitude constraint and to minimize the coordination error. Then, the study of the mechanism joining the third finger and the little finger is summarized. Finally, a prototype of the finger's abduction system is presented.

This paper was presented at the IFToMM/ASME International Workshop on Underactuated Grasping (UG2010), 19 August 2010, Montréal, Canada.

1 Introduction

This paper presents work currently underway aiming at the design of an underactuated hand for an anthropomorphic robot. Underactuation has been chosen to simplify the control of this hand and to minimize its cost in order to facilitate its use by a humanoid robot. The 16-degree-of-freedom hand will therefore need four actuators to control its closing and opening motion as well as its abduction movement. The analyses of underactuation in the fingers and thumb were already presented (Demers and Gosselin, 2009, 2010). In order to maximize the range of feasible grasps, a mechanism for the abduction of the fingers is developed here. Abduction is the action of pulling a member away from a median axis. According to Boutan and Casoli (2005), a typical grasp, the spherical grip, is associated with maximum separation of fingers "made in relation to the anatomical axis of the hand through the 3rd ray", i.e., the middle finger. Therefore, the abduction mechanism of the fingers should leave the middle finger fixed. Thereby, the thumb could perform a pinch with it when they are in opposition.

2 Prescribed abduction movements

In regard to measuring the magnitude of the spacing between the fingers, no source using a universal goniometer was found by Norkin and White (2009). For their part, Smahel and Klímová (2004) traced the contour of the fingers apart to measure the maximum angle between adjacent fingers. Also, Gurbuz et al. used an electronic inclinometer to measure active abduction of metacarpophalangeal joints (Gurbuz et al., 2006). Since no trend is apparent from these articles, we used the method proposed by Smahel and compared our results with those of other studies. We then concluded that a maximal abduction of 25° between each finger would be sufficient, which represents a range of 50° for the little finger.

It was also noted in the literature (Tubiana and Thomine, 1990; Kapandji, 2005) that the rays, the extensions of the fingers, all converge to a point at the base of the palm when the fingers are fully abducted, as illustrated in Fig. 1. Added to the fact that their width limits the minimum distance between them, it is possible to calculate the position of the axes of rotation, $O_{0,i}$, for the abduction of the metacarpals. Assuming that the distance between the centres of the fingers must be 25.4 mm and that the maximum abduction be 25°, we can calculate the distance from the meeting point p_0 of the rays on the middle finger's axis, that is 54.47mm. These dimensions are shown in Fig. 1. Furthermore, the metacarpophalangeal joints, $O_{1,i}$, in outspread position must be equidistant from the point of intersection of rays, p_0. For fingers of same

Correspondence to: C. Gosselin
(gosselin@gmc.ulaval.ca)

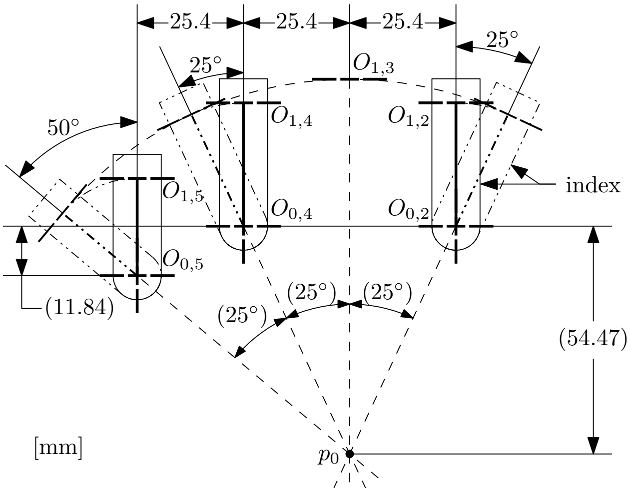

Figure 1. Abduction movement of the metacarpals.

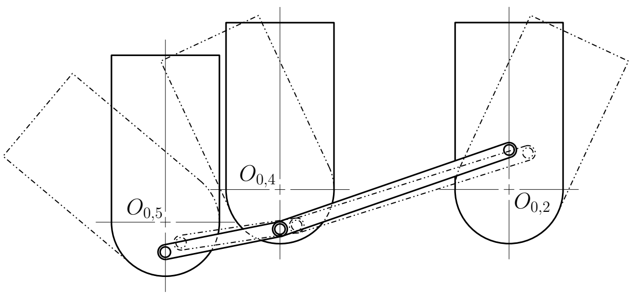

Figure 2. Linkage connecting the metacarpals.

dimension this specification allows the tips to be at the same distance during the closing, which is useful for a spherical grip. This feature is not necessary when making a cylindrical grip where the fingers are adjacent and wrapped around the object.

In order to simplify the architecture of the hand, abduction of the fingers and thumb should be performed with a single actuator. The mechanism of abduction of the thumb was presented in another article (Demers and Gosselin, 2010), but it is important to emphasize that its metacarpal is driven by a worm gear. This input can also be used to drive the abduction of the fingers. The design of the mechanism for the abduction of the fingers therefore consists in developing a link between the index and ring fingers, followed by a link between the ring and little fingers. Since simplicity and stiffness in the connection is required for a stable spherical grasp, two 4-bar mechanisms will be used, as shown in Fig. 2.

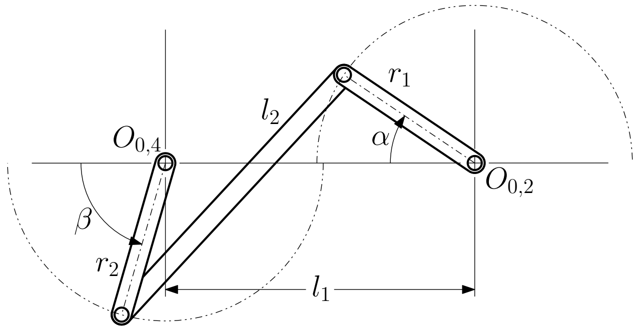

Figure 3. Linkage connecting the metacarpals of the index and ring fingers.

3 Linkage between the index and ring fingers

Since a 4-bar mechanism has been chosen to connect the index and ring fingers, it is now interesting to analyze the relationship between the input and output angles, that is to say between α and β according to Fig. 3. We must thus determine the parameters of the mechanism that will allow the ring finger to follow the abduction of the index, in other words the range of motion $\Delta\beta$ between the initial and final position of the ring finger is equal to the range of motion of the index, $\Delta\alpha$. Also, it is preferable that this abduction be performed with a somewhat synchronized motion of the fingers, so $\delta\beta \approx \delta\alpha$ during the trajectory.

With Fig. 3, it is possible to establish that

$$l_2^2 = (r_2\cos\beta + l_1 - r_1\cos\alpha)^2 + (r_1\sin\alpha + r_2\sin\beta)^2 \tag{1}$$

and using equal radii, $r_1 = r_2 = r$, one can obtain

$$A_\beta\cos\beta + B_\beta\sin\beta = C_\beta \tag{2}$$

where

$$A_\beta = \cos\alpha - \frac{l_1}{r} \tag{3}$$

$$B_\beta = -\sin\alpha \tag{4}$$

$$C_\beta = 1 + \frac{l_1^2 - l_2^2}{2r^2} - \frac{l_1}{r}\cos\alpha. \tag{5}$$

In a typical linkage synthesis application, Eq. (1) is written for a series of prescribed input-output pairs until a sufficient number of conditions is obtained. The equations are then solved using, for instance, nonlinear least squares techniques. However, in this work, only a small set of constraints will first be imposed, thereby leaving some design freedom in the problem. Then, a detailed analysis will be performed in order to explore the possibility of minimizing the coordination error throughout the motion range, without arbitrarily prescribing a large number of input-ouput points.

Equation (2) is readily solved and leads to two values of angle β associated with the input angle α for given link lengths. Since the abduction range of motion of the index and ring fingers should both be equal to 25°, thus $\Delta\beta = \Delta\alpha = 25°$. It is thus necessary to establish a relationship between these amplitudes and ratios l_1/r or l_2/r in order to synthesize a mechanism that will meet this condition.

3.1 Amplitudes of abduction

Using the initial, β_0, medial, β_1, and final, β_2, angles of the ring finger as well as those of the index, α_0, α_1 and α_2, relationships between these angles can be established.

$$\beta_2 - \beta_0 = \Delta\beta = \Delta\alpha = \alpha_2 - \alpha_0 \tag{6}$$

Consequently

$$\beta_2 = \beta_1 + \frac{\Delta\beta}{2} = \beta_1 + \frac{\Delta\alpha}{2} \tag{7}$$

$$\beta_0 = \beta_1 - \frac{\Delta\beta}{2} = \beta_1 - \frac{\Delta\alpha}{2} \tag{8}$$

$$\alpha_2 = \alpha_1 + \frac{\Delta\alpha}{2} \tag{9}$$

$$\alpha_0 = \alpha_1 - \frac{\Delta\alpha}{2}. \tag{10}$$

It is important to note that the median angles α_1 and β_1 do not necessarily occur simultaneously. Indeed, at this point, Eq. (2) is not required to be satisfied for α_1 and β_1. Equation (2) can be rewritten to highlight the constant term for a given mechanism, which leads to

$$\cos(\alpha+\beta) + \frac{l_1}{r}(\cos\alpha - \cos\beta) = 1 + \frac{l_1^2 - l_2^2}{2r^2}. \tag{11}$$

From the initial configuration (α_0, β_0) to the final one (α_2, β_2), the left hand side of Eq. (11) must always give the same result for the mechanism to be assembled. Therefore, one can write

$$\cos(\alpha_0+\beta_0) + \frac{l_1}{r}(\cos\alpha_0 - \cos\beta_0) = \cos(\alpha_2+\beta_2) + \frac{l_1}{r}(\cos\alpha_2 - \cos\beta_2). \tag{12}$$

Substituting Eq. (7) to Eq. (10) into Eq. (12), one can obtain

$$0 = -2\sin(\alpha_1+\beta_1)\sin\Delta\alpha + 2\frac{l_1}{r}(\sin\beta_1 - \sin\alpha_1)\sin\frac{\Delta\alpha}{2}. \tag{13}$$

The latter equation is satisfied if either $\Delta\alpha = 2n\pi$ where $n \in \mathbb{N}$, so the mechanism does not move or makes n turns, or $\sin(\alpha_1+\beta_1) = 0$ and $\sin\beta_1 - \sin\alpha_1 = 0$ for any l_1/r. The latter conditions are satisfied if and only if $\alpha_1 + \beta_1 = (2n-1)\pi$. Since the four-bar mechanism is assembled using the inverted branch and $\Delta\beta = \Delta\alpha$, then it follows from Eq. (7) to Eq. (10) that

$$\alpha_1 + \beta_1 = \pi \tag{14}$$

$$\alpha_0 + \beta_2 = \pi \tag{15}$$

$$\alpha_2 + \beta_0 = \pi. \tag{16}$$

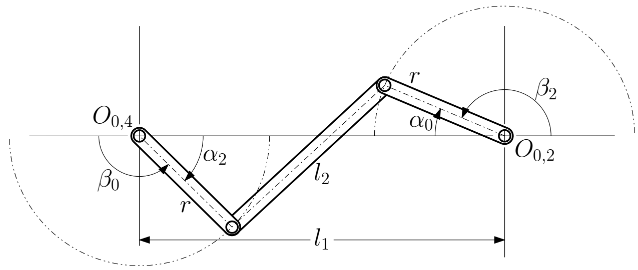

Figure 4. Linkage connecting the metacarpals of the index and ring fingers in its initial position (α_0, β_0).

Equations (15) and (16), described in Fig. 4, can then be substituted into Eq. (1), leading to

$$\left(\frac{l_2}{r}\right)^2 = \left(\frac{l_1}{r} - \cos\alpha_0 - \cos\alpha_2\right)^2 + \left(\sin\alpha_0 + \sin\alpha_2\right)^2 \tag{17}$$

which can be rewritten as

$$\left(\frac{l_2}{r}\right)^2 = \left(\frac{l_1}{r}\right)^2 - 4\frac{l_1}{r}\cos\alpha_1\cos\frac{\Delta\alpha}{2} + 4\cos^2\frac{\Delta\alpha}{2}. \tag{18}$$

For a given range of abduction $\Delta\alpha$, it is then possible to use the above equation to calculate the ratio l_2/r with l_1/r and α_1.

3.2 Minimizing the coordination error

In addition to imposing that the difference between the initial and final position of the ring finger is equal to that of the index, i.e. $\Delta\beta = \Delta\alpha$, it is required that the abduction motion of the fingers be somewhat synchronized, that is to say $\delta\beta \approx \delta\alpha$ over the motion range. It is therefore necessary to minimize the coordination error e_β between the orientation of the ring and index fingers. This can be described as the absolute difference between the angular displacements, i.e.

$$e_\beta = \left|(\beta - \beta_0) - (\alpha - \alpha_0)\right| = \left|\beta - \alpha - (\beta_1 - \alpha_1)\right| \tag{19}$$

and with Eq. (14):

$$e_\beta = \left|\beta - \alpha - \pi + 2\alpha_1\right|. \tag{20}$$

The error varies with the configuration of the mechanism, i.e. according to α and β. The parameters that can be modified in order to minimize the error e_β are l_1/r and α_1, since $\Delta\alpha$ is constrained and α varies according to $\alpha_1 - \Delta\alpha/2 \le \alpha \le \alpha_1 + \Delta\alpha/2$. The minimization of the error can be performed in several ways.

It is first interesting to trace the contours of the coordination error e_β for $\alpha_0 \le \alpha \le \alpha_2$ and various α_1 using a prescribed ratio l_1/r, as shown in Fig. 5. To minimize the error on the interval $\alpha_0 \le \alpha \le \alpha_2$, we can examine the evolution of the mean and the maximum error on this interval. Figure 6 is obtained using again $l_1/r = 5$. It can be observed in Fig. 5 that a minimum can be achieved for the error e_β. The value of α_1 for this minimum is denoted α_g in Fig. 6 and we note that

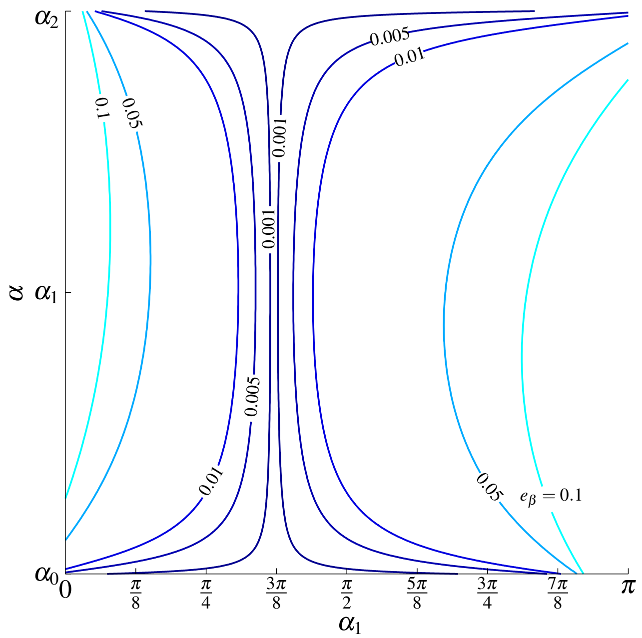

Figure 5. Coordination Error e_β as a function of the median angle α_1 for $\alpha_0 \le \alpha \le \alpha_2$ if $l_1/r = 5$.

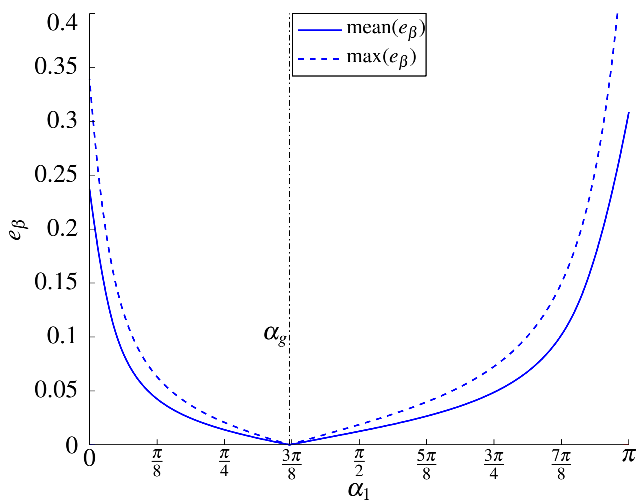

Figure 6. Mean and maximum error in the interval $\alpha_0 \le \alpha \le \alpha_2$ as a function of α_1 for $l_1/r = 5$.

the maximum as well as the average error over the interval is then minimized.

Since the trend of coordination error can be followed with its maximum value as well as its mean, it is now possible to analyze the effects of changing α_1 along with l_1/r, as shown in Fig. 7. Low levels contours (0.01, 0.025, 0.04, 0.055, 0.07, 0.085) were added to higher levels (0.1, 0.2, 0.3, 0.4, 0.5) to indicate the rapid growth of the error following the deviation from the ideal value α_g.

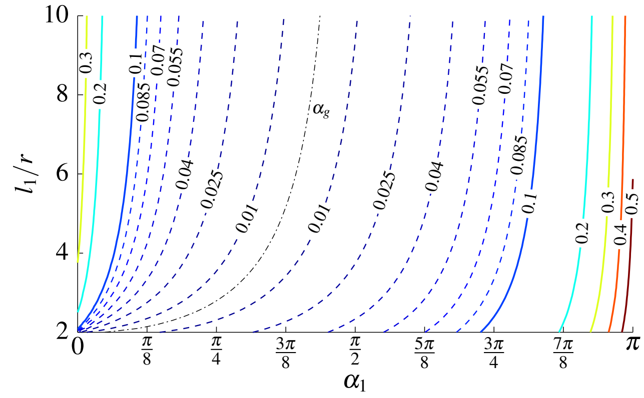

Figure 7. Maximum error in the interval $\alpha_0 \le \alpha \le \alpha_2$ as a function of α_1 and l_1/r.

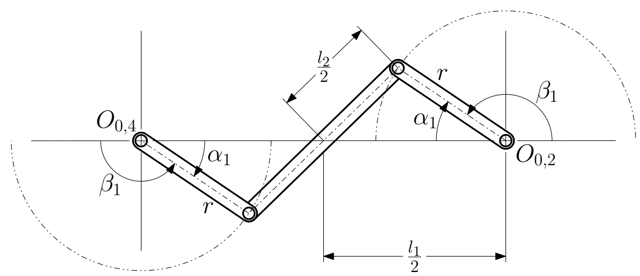

Figure 8. Linkage between the index finger and ring finger if the middle positions occur simultaneously.

Assuming that the median angles α_1 and β_1 occur simultaneously and using Eq. (14), we can conclude that the centre of the link of length l_2 is located at the centre point between the two axes of rotation as sketched in Fig. 8. It is then possible to deduce the angle α_1.

$$\cos\alpha_1 = \frac{1 + \left(\frac{l_1}{2r}\right)^2 - \left(\frac{l_2}{2r}\right)^2}{l_1/r} \tag{21}$$

Using Eq. (21), one can factor Eq. (18) into two terms to emphasize its roots

$$0 = \left[\left(\frac{l_1}{r}\right)^2 - \left(\frac{l_2}{r}\right)^2 - 4\cos\frac{\Delta\alpha}{2}\right]\left[1 - \cos\frac{\Delta\alpha}{2}\right] \tag{22}$$

where we find again the trivial case $\Delta\alpha/2 = 2n\pi$. Besides, it is obvious that an equation to calculate l_2/r can be obtained from the first term, which gives:

$$\frac{l_2}{r} = \sqrt{\left(\frac{l_1}{r}\right)^2 - 4\cos\frac{\Delta\alpha}{2}} \tag{23}$$

and we can finally change Eq. (21) to calculate the angle α_1 as a function of $\Delta\alpha/2$ and l_1/r.

$$\cos\alpha_1 = \frac{1 + \cos\frac{\Delta\alpha}{2}}{l_1/r} \tag{24}$$

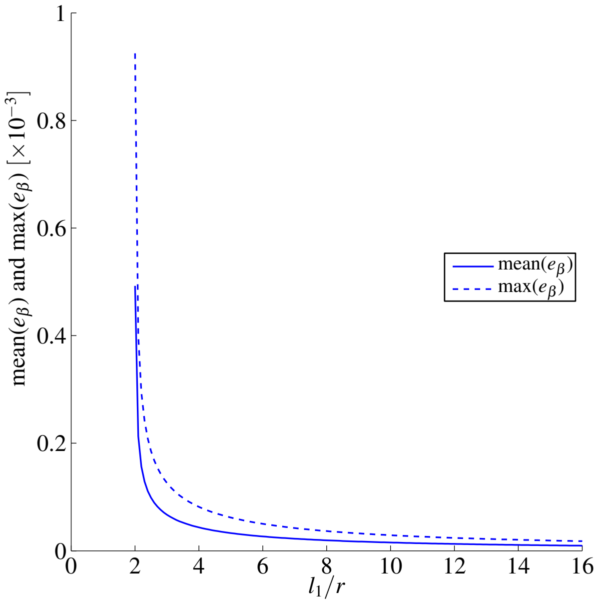

Figure 9. Mean and maximum error in the interval $\alpha_0 \le \alpha \le \alpha_2$ according to l_1/r.

The median angle α_1 obtained must be used if one wants to reduce the coordination error between the orientation of the ring finger and index finger. It is this angle, i.e. α_g, which is indicated on Fig. 6 and Fig. 7. Indeed, if we use $\Delta\alpha = 25°$ and $l_1/r = 5$, we obtain $\alpha_1 \approx 1.164 \approx 3\pi/8$, which is the value of α_g already found for these parameters.

Since Eq. (24) gives a relationship between the two parameters of the optimization, minimizing the error e_β on the interval $\alpha_0 \le \alpha \le \alpha_2$ depends now only on the ratio l_1/r. It is then possible to obtain Fig. 9 by tracing the evolution of the mean and the maximum error following this parameter. It is obvious that for values of $l_1/r > 3$ the maximum and average of the error e_β become negligible (max $(e_\beta) < 0.13 \times 10^{-3}$). Moreover, from $l_1/r = 5$, the slope of the curve max (e_β) remains greater than -0.015×10^{-3}. Since the distance l_1 between the axes of the index and ring fingers is equal to 50.8 mm, we can assume that a ratio $l_1/r = 5.08$ is feasible in practice, because the distance between two joints is then $r = 10$ mm. For guidance, we obtain $l_2/r \approx 4.68$, thus $l_2 \approx 46.8$ mm and $\alpha_1 \approx 1.171$.

The error obtained using this ratio is presented in Fig. 10 on a logarithmic scale. One can observe that the error is minimized over the interval $\alpha_0 \le \alpha \le \alpha_2$. In fact, the magnitude of the error generated is negligible in practice. Moreover, since we have imposed $\Delta\beta = \Delta\alpha$, we obtain $e_\beta = 0$ when $\alpha = \alpha_0$ and $\alpha = \alpha_2$. The error is also zero when $\alpha = \alpha_1$, because this angle is now calculated so that β_1 is achieved simultaneously with α_1. With Eq. (19), it is obvious that the error is null if one uses $\alpha = \alpha_1$ and $\beta = \beta_1$. Finally, the evolution of the angle β as a function of the angle α using $l_1/r = 5$ is plotted in Fig. 11.

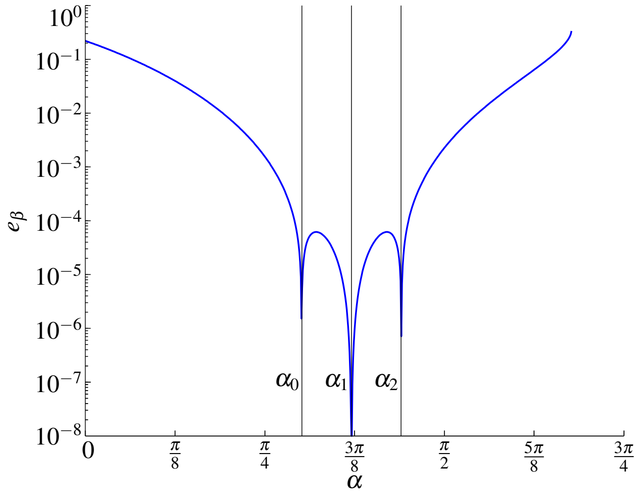

Figure 10. Error e_β as a function of α with $l_1/r = 5$.

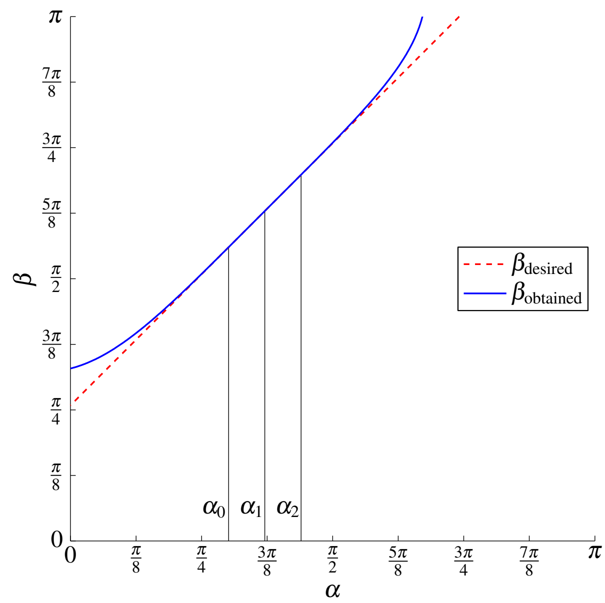

Figure 11. Angle β desired and obtained as a function of angle α with $l_1/r = 5$.

4 Linkage between the ring finger and the little finger

Since the parameters of the linkage between the index and ring fingers are fixed, it is now possible to analyze the linkage between the ring and little fingers, as shown in Fig. 12.

By following the same approach used to analyze the four-bar mechanism connecting the index and ring fingers, it is possible to determine from Fig. 12 that

$$l_4^2 = (r_3\cos\gamma + l_3 - r_2\cos\beta)^2 + (r_3\sin\gamma + l_5 - r_2\sin\beta)^2 \tag{25}$$

which yields

$$A_\gamma\cos\gamma + B_\gamma\sin\gamma = C_\gamma \tag{26}$$

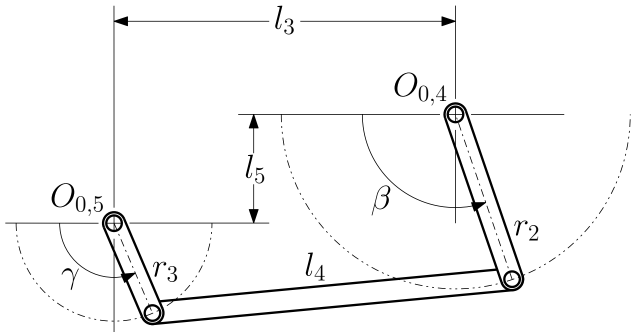

Figure 12. Linkage between the ring finger and the little finger metacarpals.

with

$$A_\gamma = 2r_3(r_2\cos\beta - l_3) \tag{27}$$
$$B_\gamma = 2r_3(r_2\sin\beta - l_5) \tag{28}$$
$$C_\gamma = r_2^2 + r_3^2 + l_3^2 + l_5^2 - l_4^2 - 2r_2(l_3\cos\beta + l_5\sin\beta). \tag{29}$$

Equation (26) is readily solved for γ if all other parameters are given. Since β_1 and r_2 of this linkage are equal to β_1 and r_2 of the previous linkage in order to simplify the mechanism, it is preferable to use links of different lengths in order to keep parameter r_3 for the optimization.

Again, the median angle γ_1 giving the lowest error is first established, which will subsequently be used to determine r_3 and l_4. Since the amplitude of the range of motion for the little finger is 50°, we have $\Delta\gamma = 2\Delta\beta = 50°$.

4.1 Amplitudes of abduction

Initial, γ_0, medial, γ_1, and final, γ_2, angles of the little finger are assumed to be similar to those of the ring finger, β_0, β_1, β_2. This allows to establish relations similar to those derived in the previous section:

$$\gamma_2 - \gamma_0 = \Delta\gamma = 2\Delta\beta = 2(\beta_2 - \beta_0) \tag{30}$$

thus

$$\gamma_2 = \gamma_1 + \frac{\Delta\gamma}{2} = \gamma_1 + \Delta\gamma \tag{31}$$
$$\gamma_0 = \gamma_1 - \frac{\Delta\gamma}{2} = \gamma_1 - \Delta\gamma \tag{32}$$

$$\beta_2 = \beta_1 + \frac{\Delta\beta}{2} \tag{33}$$
$$\beta_0 = \beta_1 - \frac{\Delta\beta}{2}. \tag{34}$$

Again, the median angles β_1 and γ_1 do not necessarily occur simultaneously. Following the same method as in the previous case, it is possible to rewrite Eq. (26) as $g(\beta,\gamma) = l_6$ where

$$\begin{aligned} g(\beta,\gamma) &= r_2 r_3\cos(\beta-\gamma) + l_3(r_2\cos\beta - r_3\cos\gamma) \\ &\quad + l_5(r_2\sin\beta - r_3\sin\gamma) \end{aligned} \tag{35}$$
$$l_6 = \frac{r_2^2 + r_3^2 + l_3^2 + l_5^2 - l_4^2}{2}. \tag{36}$$

Since l_6 is constant for a given mechanism, the function $g(\beta,\gamma)$ must also be constant. Consequently, it is possible to use the two positions where the angles are known, i.e., the initial (β_0,γ_0) and final (β_2,γ_2) configurations, to find a relationship between γ_1 and r_3 not involving l_4.

One has:

$$0 = g(\beta_0,\gamma_0) - g(\beta_2,\gamma_2) \tag{37}$$

which can be rewritten as

$$\begin{aligned} 0 &= r_2\Big(r_3\sin(\gamma_1-\beta_1) + l_3\sin\beta_1 - l_5\cos\beta_1\Big)\sin(\Delta\beta/2) \\ &\quad + r_3\Big(l_5\cos\gamma_1 - l_3\sin\gamma_1\Big)\sin\Delta\beta. \end{aligned} \tag{38}$$

If $\sin(\Delta\beta/2) \neq 0$, i.e. $\Delta\beta \neq 2n\pi$ where $n \in \mathbb{N}$, which implies that the mechanism does not move or makes n complete turns, then it is possible to obtain

$$\begin{aligned} 0 &= r_2\Big(r_3\sin\gamma_1\cos\beta_1 - r_3\cos\gamma_1\sin\beta_1 + l_3\sin\beta_1 - l_5\cos\beta_1\Big) \\ &\quad + r_3\Big(l_5\cos\gamma_1 - l_3\sin\gamma_1\Big)2\cos(\Delta\beta/2) \end{aligned} \tag{39}$$

and finally

$$\frac{r_2}{r_3} = \frac{r_2\sin\beta_1 - 2l_5\cos\frac{\Delta\beta}{2}}{l_3\sin\beta_1 - l_5\cos\beta_1}\cos\gamma_1 + \frac{-r_2\cos\beta_1 + 2l_3\cos\frac{\Delta\beta}{2}}{l_3\sin\beta_1 - l_5\cos\beta_1}\sin\gamma_1. \tag{40}$$

Knowing the values of $\Delta\beta$, β_1, r_2, l_3 and l_5, it is possible to use Eq. (40) to calculate r_3 depending of γ_1 and vice versa.

With r_3 and γ_1, it is then possible to calculate l_4 using the loop closure equation of the mechanism in the initial position (β_0,γ_0):

$$\begin{aligned} l_4^2 &= (r_3\cos(\gamma_1-\Delta\beta) + l_3 - r_2\cos(\beta_1 - \Delta\beta/2))^2 \\ &\quad + (r_3\sin(\gamma_1-\Delta\beta) + l_5 - r_2\sin(\beta_1-\Delta\beta/2))^2. \end{aligned} \tag{41}$$

This allows to plot the lengths r_3 and l_4 in terms of γ_1 as presented in Fig. 13, where $\Delta\beta = 25°$, $\beta_1 = 1.97$, $r_2 = 10$ mm, $l_3 = 25.4$ mm and $l_5 = 11.8$ mm were used.

Knowing for γ_1 the value of r_3 and l_4, it is possible to calculate angle γ using Eq. (26) as well as the coordination error e_γ between the little finger and the ring finger, where

$$e_\gamma = \big|(\gamma-\gamma_0) - 2(\beta-\beta_0)\big| = \big|\gamma - 2\beta - (\gamma_1 - 2\beta_1)\big|. \tag{42}$$

It is finally possible to see the coordination error on the interval $\beta_0 \leq \beta \leq \beta_2$ according to the median angle γ_1 chosen, as shown in Fig. 14. Again, it is interesting to see the evolution of the mean and the maximum error on the useful range of β: this can be done with Fig. 15. The error is then minimized when $\gamma_1 = \gamma_{1g}$, which represents the median angle for which the error becomes zero when $\beta = \beta_1$, as seen in Fig. 14.

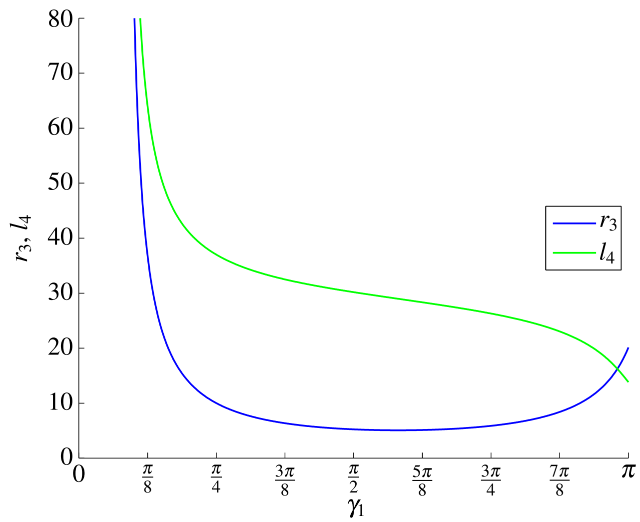

Figure 13. Lengths r_3 and l_4 as a function of angle γ_1.

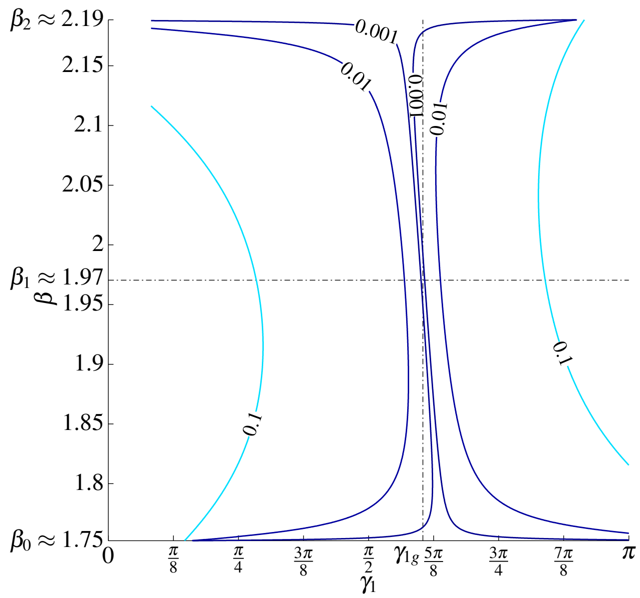

Figure 14. Error e_γ as a function of γ_1 and β.

One can obtain γ_{1g} with $0 = g\left(\beta_1, \gamma_{1g}\right) - g(\beta_0, \gamma_0)$, i.e.,

$$\begin{aligned} 0 &= r_2 r_3 \cos\left(\beta_1 - \gamma_{1g}\right) + l_3\left(r_2\cos\beta_1 - r_3\cos\gamma_{1g}\right) \\ &\quad + l_5\left(r_2\sin\beta_1 - r_3\sin\gamma_{1g}\right) - r_2 r_3\cos(\beta_0 - \gamma_0) \\ &\quad - l_3(r_2\cos\beta_0 - r_3\cos\gamma_0) - l_5(r_2\sin\beta_0 - r_3\sin\gamma_0) \end{aligned} \tag{43}$$

which can be rearranged as

$$\begin{aligned} 0 &= \cos\gamma_{1g}\Big(r_2\big(\cos\beta_1 - \cos\beta_2\big) - l_3\big(1-\cos\Delta\beta\big) - l_5\sin\Delta\beta\Big) \\ &\quad + \sin\gamma_{1g}\Big(r_2\big(\sin\beta_1 - \sin\beta_2\big) + l_3\sin\Delta\beta - l_5\big(1-\cos\Delta\beta\big)\Big) \\ &\quad + \frac{r_2}{r_3}\Big(l_3\cos\beta_1 - l_3\cos\beta_0 + l_5\sin\beta_1 - l_5\sin\beta_0\Big) \end{aligned} \tag{44}$$

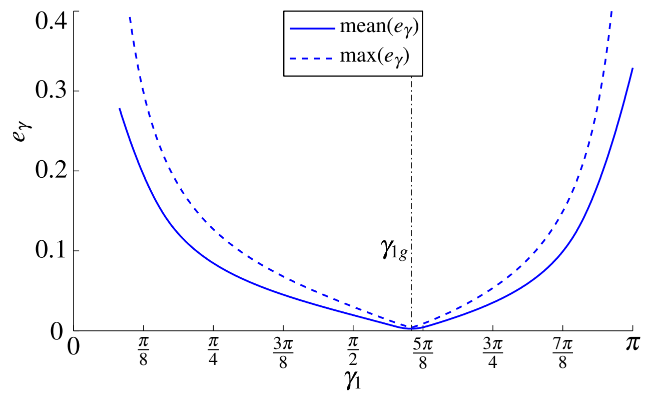

Figure 15. Mean and maximum error in the interval $\beta_0 \le \beta \le \beta_2$ as a function of γ_1.

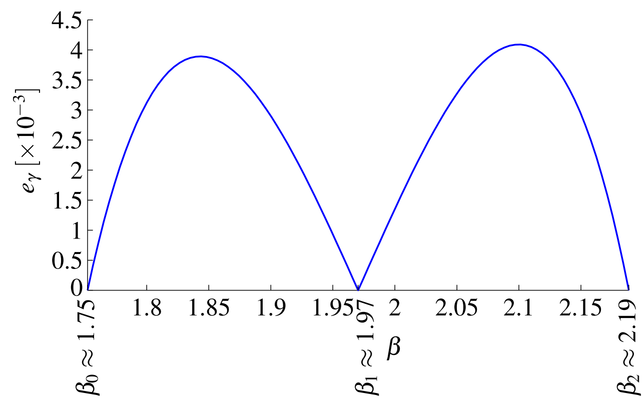

Figure 16. Error e_γ as a function of angle β.

then, substituting Eq. (40) into Eq. (44), one obtains:

$$A_{\gamma_{1g}}\cos\gamma_{1g} + B_{\gamma_{1g}}\sin\gamma_{1g} = 0. \tag{45}$$

where

$$\begin{aligned} A_{\gamma_{1g}} &= r_2\big(\cos\beta_1 - \cos\beta_2\big) - l_3\big(1-\cos\Delta\beta\big) - l_5\sin\Delta\beta \\ &\quad + d_{\gamma_{1g}}\big(r_2\sin\beta_1 - 2l_5\cos\Delta\beta/2\big) \end{aligned} \tag{46}$$

$$\begin{aligned} B_{\gamma_{1g}} &= r_2\big(\sin\beta_1 - \sin\beta_2\big) + l_3\sin\Delta\beta - l_5\big(1-\cos\Delta\beta\big) \\ &\quad + d_{\gamma_{1g}}\big(-r_2\cos\beta_1 + 2l_3\cos\Delta\beta/2\big) \end{aligned} \tag{47}$$

$$d_{\gamma_{1g}} = \frac{l_3(\cos\beta_1 - \cos\beta_0) + l_5(\sin\beta_1 - \sin\beta_0)}{l_3\sin\beta_1 - l_5\cos\beta_1}. \tag{48}$$

which is readily solved for γ_{1g}. Using the same parameters as used for Fig. 13, we obtain $\gamma_{1g} \approx 1.90$ and the associated values $r_3 \approx 5.1$ mm and $l_4 \approx 28.6$ mm. The error e_γ is presented in Fig. 16. One can observe that the error is zero at $\beta = \beta_0, \beta_1$ and β_2. Finally, the angle γ is plotted in Fig. 17 as a function of angle β.

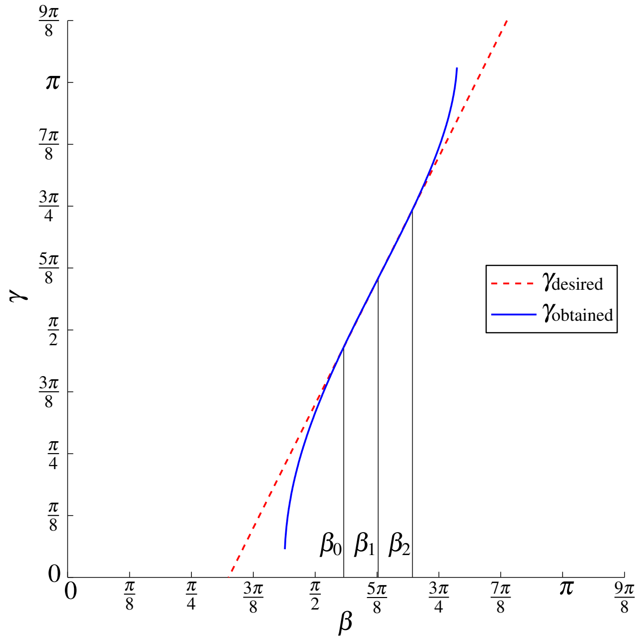

Figure 17. Angle γ desired and obtained according to β.

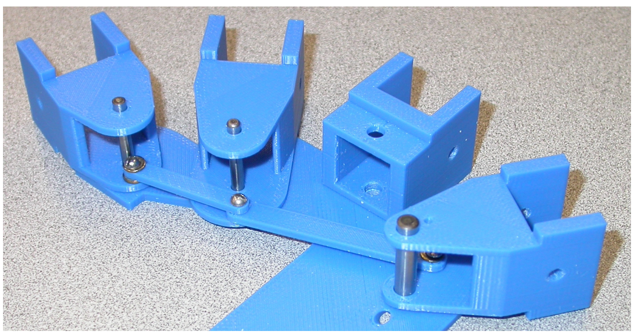

Figure 18. Prototype of the finger abduction system.

5 Prototype

Using the values found in this study, the prototype shown in Fig. 18 was built with rapid prototyping. One can note the similarity with the schematic presented in Fig. 2, on which the fixed middle finger metacarpal has been added. Again, the input consisting of a worm gear connecting with the index metacarpal is not shown. This mechanism will enhance the range of feasible grasps of the underactuated hand without significantly increasing its complexity.

6 Conclusions

The kinematic design of the finger abduction mechanism for an underactuated anthropomorphic robotic hand has been presented. The parameters of the linkage between the index finger and the third finger has been analyzed, followed by those of the linkage between the ring finger and the little finger. We therefore obtain a simple architecture that minimizes the coordination error among the abduction angles.

A robotic hand using this abduction mechanism is being built. It will use underactuation within its fingers and among them and will be tendon-driven (Demers and Gosselin, 2009, 2010). Testing of its grasping capabilities will then be conducted in order to validate this design.

Acknowledgements. This work was supported by the Fonds québécois de la recherche sur la nature et les technologies (FQRNT), the Natural Sciences and Engineering Research Council of Canada (NSERC) as well as by the Canada Research Chair Program.

Edited by: J. L. Herder
Reviewed by: two anonymous referees

References

Boutan, M. and Casoli, V.: Mains & Préhensions entre fonctions et anatomie, Sauramps médical, Montpellier, 2005.

Demers, L.-A. A. and Gosselin, C.: Kinematic design of an ejection-free underactuated anthropomorphic finger, in: Proceedings of the IEEE International Conference on Robotics and Automation (ICRA 2009), Kobe, Japan, 12–17 May 2009, 2086–2091, 2009.

Demers, L.-A. A. and Gosselin, C.: Kinematic design of a thumb metacarpal for an anthropomorphic robotic hand, in: Proceedings of the ASME International Design Engineering Technical Conferences (IDETC 2010), Montréal, Canada, 15–18 August 2010.

Gurbuz, H., Mesut, R., and Nesrin Turan, F.: Measurement of active abduction of metacarpophalangeal joints via electronic digital incinometric technique, Ital. J. Anat. Embryol., 111, 9–14, 2006.

Kapandji, A. I.: Physiologie articulaire : schémas commentés de mécanique humaine, Vol. 1, Maloine, 6 Edn., 2005.

Norkin, C. C. and White, D. J.: Measurement of Joint Motion: A Guide to Goniometry, Philadelphia, 4 Edn., 2009.

Smahel, Z. and Klímová, A.: The influence of age and exercise on the mobility of hand joints: 1: Metacarpophalangeal joints of the three-phalangeal fingers, Acta Chir. Plast., 46, 81–88, 2004.

Tubiana, R. and Thomine, J. M.: La main : Anatomie fonctionnelle et examen clinique, Masson, Paris, 1990.